Int. J. Solids Structures Vol. 16, pp. 1017–1035
Pergamon Press Ltd., 1980. Printed in Great Britain

UNSTABLE GROWTH OF TENSION CRACKS IN BRITTLE SOLIDS: STABLE AND UNSTABLE BIFURCATIONS, SNAP-THROUGH, AND IMPERFECTION SENSITIVITY

S. NEMAT-NASSER,† Y. SUMI, ‡ and L. M. KEER§

Department of Civil Engineering, The Technological Institute, Northwestern University, Evanston, IL 60201, U.S.A.

(*Received* 30 *July* 1979; *in revised form* 7 *December* 1979)

Abstract—The growth pattern of a system of tension cracks in a linearly elastic brittle solid, may undergo abrupt changes, e.g. some cracks may stop or actually close, as others snap to finitely longer lengths. For the growth regime of a system of straight edge cracks in plane strain, the concepts of fundamental equilibrium path, stable and unstable bifurcation points and snap-through critical point are introduced and the corresponding behaviors are studied. In particular, it is shown that instabilities of this kind are highly imperfection-sensitive in the sense that, for example, a small material inhomogeneity can decrease by a large amount the critical value of the load parameter at which a growth regime abruptly changes to a new one. For thermally induced tension edge cracks in an infinite strip of finite width, numerical results are presented and various aspects of the theory are illustrated. For the calculation the new combined analytic and finite-element solution method recently given by the authors is employed.

1. INTRODUCTION

Tension cracks often form in brittle solids, because of a variety of mechanisms, such as nonuniform shrinkage due to loss of moisture or due to creep deformation, nonuniform temperature fields, radiation induced nonuniform volume changes and others. Mechanisms of this kind are "strain-controlled," in the sense that at each stage of crack growth, the total elastic strain energy available to each crack is finite. Upon crack extension, the elastic energy is released and therefore the crack growth is self-arresting.

However, in a suitable setting, two or several tension cracks may interact which may lead to abrupt changes in their growth pattern. For example, as cracks grow with a continuous supply of elastic energy (e.g. because of continuous loss of moisture or heat), a critical state may be reached, where some cracks stop growing, as others grow at a faster rate. Another example of a change in the growth pattern is when some cracks actually snap closed while others extend by a finite amount. Unstable crack growth of this kind was first examined by Nemat-Nasser[1,2] and with detailed calculations by Nemat-Nasser¶ *et al.*[3] and Keer *et al.*[4]. Although a number of interesting and essential features pertaining to this class of problems have been delineated in the above references, several other key questions have been left unresolved. A question of considerable practical improtance is the effect of small imperfections which are bound to exist in real situations. As is now well-known, stability of many elastic structures is imperfection sensitive, in the sense that small geometric or other imperfections may reduce by a large amount the value of the critical load at which the structure becomes unstable. This has been examined in a pioneering work by Von Karman and Tsien[6] and has since been thoroughly explored both theoretically and experimentally by a number of other researchers; for references and discussions, see Hutchinson and Koiter[7], Chilver[8] and Roorda[9]. We shall show in this paper that for interacting tension cracks, also, small imperfections can substantially reduce the level of straining at which a crack growth pattern becomes unstable. In fact, for the example used to illustrate the basic results, it turns out that a 3% imperfection in material parameters reduces the critical value of the "load parameter" by more than 20%.

†Professor of Civil Engineering and Applied Mathematics.
‡Visiting Scholar, on leave from Yokohama National University, Yokohama, Japan.
§Professor of Civil and Mechanical Engineering.
¶The basic theory has been presented in an internal technical report by Keer *et al.*[5].

The theory is presented for a system of parallel edge cracks in plane strain, induced in an elastic half-plane by the removal of heat at the free surface. This problem arises in consideration of heat extraction from hot dry rock masses, a project which recently has been initiated and to a large extent, successfully implemented at the Los Alamos Scientific Laboratory in New Mexico (for discussion and references, see Nemat-Nasser *et al.*[3, 10]).

This paper is organized in the following manner. The basic problem used for illustration is defined in Section 2. The theory is presented in Section 3, where the notions of fundamental equilibrium path, stable and unstable bifurcation points, snap-through critical point and imperfection sensitivity are introduced. Numerical results are then presented in Section 4, for an infinite strip of finite width containing equally spaced edge cracks at both edges and the entire history of growth pattern of these cracks is traced to the point of failure at which *some* of the cracks emanating from opposite edges run into each other, causing splitting of the strip into pieces.

For the actual analysis it is possible to use a method similar to that employed in[3]. Here, however, we shall use the novel analysis scheme recently proposed by the present authors[11], which combines analytical calculations with a finite-element approach, and which leads to a rather effective solution procedure. For the sake of completeness, a brief summary of this method is presented in Appendix A.

2. STATEMENT OF PROBLEM

In[3, 4] an homogeneous isotropic elastic half-plane which is initially at a uniform temperature, T_0, and is then continuously cooled at its free surface, has been considered. Because of this cooling, a thermal boundary layer of thickness δ, measured from the free surface along its normal, develops in the solid. This may then lead to the formation of tension cracks emanating perpendicularly from the free surface of the half-plane. The authors in[3, 4] confine attention to a state of *plane strain*, assume a set of initially equally spaced edge-cracks and use for illustration the following temperature profiles; see Fig. 1:

$$T = 0 \quad \text{for} \quad 0 \le y \le \delta/(n+1),$$

$$T = \frac{T_0}{2}\left[1 - \cos \pi \frac{y(n+1) - \delta}{n\delta}\right] \quad \text{for} \quad \delta/(n+1) \le y \le \delta,$$

$$T = T_0 \quad \text{for} \quad \delta \le y, \tag{2.1}$$

where $n = 0.5$ is used (see Fig. 1b); and

$$T = T_0 \operatorname{erf}\left[\frac{y\sqrt{3}}{\delta}\right] \quad y \ge 0, \tag{2.2}$$

where $\operatorname{erf}(x) = \dfrac{2}{\sqrt{\pi}} \displaystyle\int_0^x e^{-u^2} du$ (see Fig. 1a).

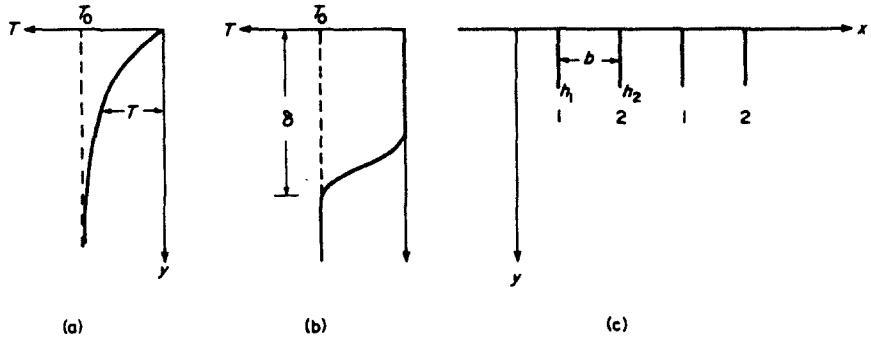

Fig. 1. (a) Temperature profile eqn (2.2); (b) temperature profile eqn (2.1); (c) half-plane with equally spaced cracks.

The temperature profile (2.2) corresponds to the case where the solid has a uniform initial temperature T_0 and then its free surface $y = 0$ is brought to zero temperature at time $t = 0$ and kept zero thereafter, losing heat by conductive heat transfer only. In this case, it can be shown that $\delta = [tk/\rho C]^{\frac{1}{2}}$, where t is time, k is the conductivity, ρ is the mass-density, and C is the heat capacity of the solid. The temperature profile (2.1), on the other hand, attempts to include, in an approximate manner, the effect of heat transfer by convection when heat is removed by means of water which moves through the cracks. For application to geothermal energy extraction, the two profiles may be regarded as limiting cases, and therefore useful for obtaining good estimates; see [10].

Initially, the cracks are all equal in length, and grow in a stable manner, as the thickness of the thermal layer, δ, is increased; δ is used as a measure of the load parameter. As long as the crack spacing b is large compared with the common crack length h, there is very weak interaction between adjacent cracks, and such a crack growth pattern is inherently stable. In this case, each crack may be regarded as an isolated one and since for a fixed δ, there is a fixed amount of elastic energy available, an extension of a crack at constant δ would release a certain amount of elastic energy, which results in a reduction of the corresponding stress intensity factor at the crack tip, and therefore crack growth will be arrested. If K is the stress intensity factor, then we have, in this case, $\partial K/\partial h < 0$; see Fig. 3 of [3].

As the common crack length increases with increasing δ the interaction between adjacent cracks becomes more important. In Fig. 2 two interacting cracks are shown in a unit cell, with h_1 and h_2 as their corresponding lengths, and K_1 and K_2 the stress intensity factors; the critical value of the stress intensity factor is K_c. In [3] the following results have been obtained and numerically illustrated.

The equilibrium regime

$$h_1 = h_2 \quad \text{and} \quad K_1 = K_2 = K_c \tag{2.3}$$

is stable as long as

$$\frac{\partial K_1}{\partial h_1} = \frac{\partial K_2}{\partial h_2} < 0, \tag{2.4}$$

and it is unstable for

$$\frac{\partial K_1}{\partial h_1} = \frac{\partial K_2}{\partial h_2} > 0, \tag{2.5}$$

the critical state corresponding to

$$\frac{\partial K_1}{\partial h_1} = \frac{\partial K_2}{\partial h_2} = 0. \tag{2.6}$$

When the critical state (2.6) is reached, one crack (say, crack 2) stops growing, as the other crack extends spontaneously (i.e. without change in δ) by an infinitesimal amount. As the load

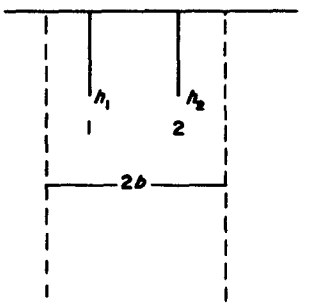

Fig. 2. A typical unit cell with two interacting cracks.

parameter is increased, crack 2 remains stationary while crack 1 grows at a faster rate. During this process, K_2 continues to decrease with increasing δ and for temperature profile (2.1), it actually becomes zero at a new critical state, after which crack 2 snaps closed, while crack 1 extends by an additional finite amount.

In a recent work, Sumi *et al.*[11] have shown that, before the critical state corresponding to (2.6) is reached, there are infinitely many stable critical states, at each of which two distinct crack growth patterns become possible: (1) equal crack growth regime defined by (2.3); and (2) a crack growth regime corresponding to

$$dh_1 > 0, dh_2 = 0, K_1 = K_2, K_2 \leq K_c, \tag{2.7}$$

i.e. one crack remaining stationary, as the other crack grows with increasing δ. These and related results are discussed in the following section.

3. CRITICAL STATES AND POST-CRITICAL BEHAVIOR

3.1 *Fundamental equilibrium path*

Consider the h_1, h_2, δ-space; Fig. 3. The *fundamental equilibrium path* in this space is the locus of points for which (2.3) holds. In Fig. 3 this is denoted by curve AB_uB. Points on this curve define equilibrium states, not all of which are stable.

3.2 *Stable bifurcation points*

When the common crack length, $h = h_1 = h_2$, is small relative to the crack spacing, the two cracks in the unit cell of Fig. 2 have a weak interaction. In this case, if at *constant* h_2 and δ, h_1 is increased

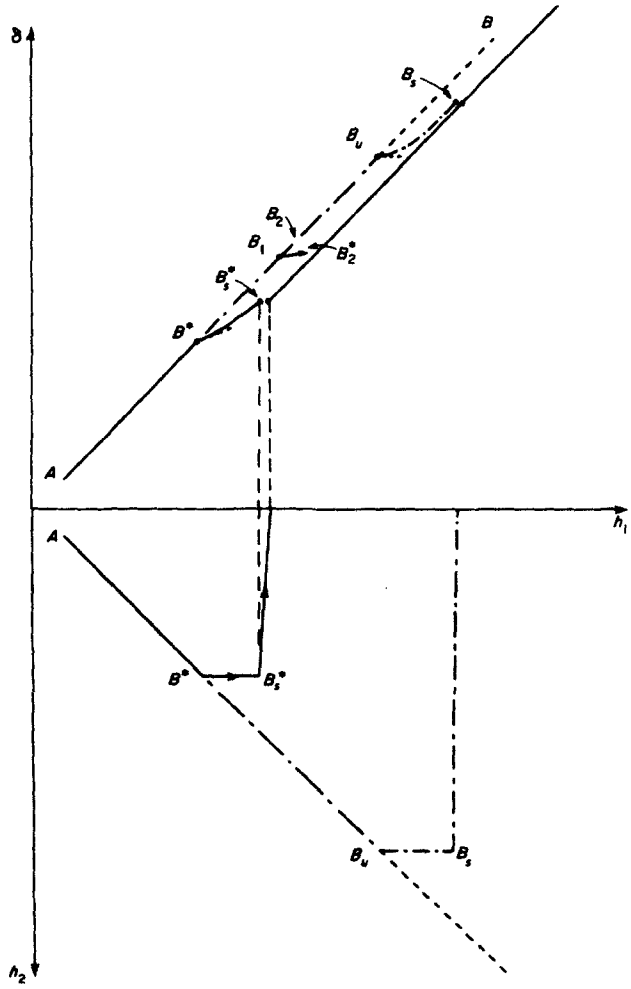

Fig. 3. Various equilibrium states for two interacting cracks: B^* is stable and B_u an unstable bifurcation point; B_s^* and B_s are snap-through critical points.

by an infinitesimal amount, the stress field will be *released* at both crack tips, and therefore, $\partial K_1/\partial h_1 < 0$ and $\partial K_2/\partial h_1 < 0$. the weak interaction then implies that the stress is released more at crack 1 than at crack 2, because of the extension of crack 1, while keeping h_2 and δ fixed. Hence, we must have $|\partial K_2/\partial h_1| < |\partial K_1/\partial h_1|$. For this regime we have

$$\frac{\partial K_1}{\partial h_1} = \frac{\partial K_2}{\partial h_2} < \frac{\partial K_1}{\partial h_2} = \frac{\partial K_2}{\partial h_1} < 0, h_1 = h_2. \tag{3.1}$$

The only possible crack extension regime then is defined by (2.3), namely the fundamental equilibrium path.

To prove this assertion, first observe that since $K_1 = K_1(h_1, h_2, \delta)$,

$$\begin{aligned} dK_1 &= \frac{\partial K_1}{\partial h_1} dh_1 + \frac{\partial K_1}{\partial h_2} dh_2 + \frac{\partial K_1}{\partial \delta} d\delta, \\ dK_2 &= \frac{\partial K_2}{\partial h_1} dh_1 + \frac{\partial K_2}{\partial h_2} dh_2 + \frac{\partial K_2}{\partial \delta} d\delta. \end{aligned} \tag{3.2}$$

Now, for $d\delta > 0$ and $dh_1 > 0$, i.e. $dK_1 = 0$, obtain

$$d\delta = -\left(\frac{\partial K_1}{\partial h_1} dh_1 + \frac{\partial K_1}{\partial h_2} dh_2\right) / \frac{\partial K_1}{\partial \delta}, \tag{3.3}$$

and, upon substitution into $(3.2)_2$, arrive at

$$dK_2 = \left(\frac{\partial K_1}{\partial h_2} - \frac{\partial K_1}{\partial h_1}\right)\left(1 - \frac{dh_2}{dh_1}\right) dh_1, \tag{3.4}$$

where, since $h_1 = h_2$, and since there is complete symmetry in this case, condition $\partial K_1/\partial \delta = \partial K_2/\partial \delta$ is used.

For $dh_1 = dh_2$, (3.4) yields $dK_2 = 0$, and hence $K_2 = K_c$: the state remains on the fundamental equilibrium path. Suppose now, $dh_2 \neq dh_1$, and assume $dh_2 > dh_1$. Then from (3.1) and (3.4) it follows that $dK_2 < 0$, and hence dh_2 must be equal to zero, which is a contradiction. Moreover, if we assume $0 \leq dh_2 < dh_1$, we obtain $dK_2 > 0$, which is impossible, since K_2 cannot exceed its critical value K_c. Hence, as long as (3.1) holds, incremental crack extension satisfies $dh_1 = dh_2$, and the state remains on the fundamental equilibrium path AB.

As the two cracks in Fig. 2 grow with increasing δ, their interaction becomes more important and when their common length is large enough, then a point may be reached at which, with h_2 and δ kept constant, an infinitesimal *extension* of crack 1 *decreases* the stress intensity factors at crack 2 and crack 1 by an equal amount. This defines a *critical point* on the fundamental equilibrium path. It is a *stable bifurcation point*, and is characterized by the condition

$$\frac{\partial K_1}{\partial h_1} = \frac{\partial K_2}{\partial h_2} = \frac{\partial K_1}{\partial h_2} = \frac{\partial K_2}{\partial h_1} < 0, h_1 = h_2. \tag{3.5}$$

To see that the state associated with (3.5) is indeed critical, observe that equilibrium requires $dK_1 = dK_2 = 0$ for $d\delta > 0$, and hence (3.2) yields

$$\begin{aligned} dh_1 &= \left(\frac{\partial K_2}{\partial h_1}\frac{\partial K_2}{\partial \delta} - \frac{\partial K_1}{\partial h_1}\frac{\partial K_1}{\partial \delta}\right) d\delta / \left\{\left(\frac{\partial K_1}{\partial h_1}\right)^2 - \left(\frac{\partial K_1}{\partial h_2}\right)^2\right\}, \\ dh_2 &= \left(\frac{\partial K_2}{\partial h_1}\frac{\partial K_1}{\partial \delta} - \frac{\partial K_1}{\partial h_1}\frac{\partial K_2}{\partial \delta}\right) d\delta / \left\{\left(\frac{\partial K_1}{\partial h_1}\right)^2 - \left(\frac{\partial K_1}{\partial h_2}\right)^2\right\}. \end{aligned} \tag{3.6}$$

Therefore uniqueness is lost when (3.5) is satisfied. On the fundamental equilibrium path in Fig. 3, this point is denoted by B^*. On this same path, points above B^* (but below B_u) satisfy the following conditions:

$$0>\frac{\partial K_1}{\partial h_1}=\frac{\partial K_2}{\partial h_2}>\frac{\partial K_1}{\partial h_2}=\frac{\partial K_2}{\partial h_1}, \quad h_1=h_2, \tag{3.7}$$

and hence correspond to stable states. However, each one of these points defines a *stable bifurcation point* from which another equilibrium path emanates.

In the immediate neighborhood of the fundamental path, these bifurcated paths characterize states with smaller total stored elastic energy per unit cell, and hence define more stable states than the corresponding ones (for the same δ) on the fundamental equilibrium path. We shall prove this assertion in the sequel, but first we shall show the existence of these stable bifurcated equilibrium paths.

To this end consider a typical point on the fundamental equilibrium path above B^*, say, point B_1 in Fig. 3. At this point, conditions (3.7) hold. Consider now an increase in the load parameter, $d\delta>0$. If equal crack growth is assumed, then point B_2 on the fundamental equilibrium path will be attained and we will have

$$h_1(B_2)=h_2(B_2)=h_1(B_1)+dh_1=h_2(B_1)+dh_2,$$
$$dh_1=dh_2>0, \quad dK_1=dK_2=0, \quad K_1(B_2)=K_2(B_2)=K_c; \tag{3.8}$$

here $h_1(B_2)$, for example, denotes the length of crack 1 at the state corresponding to B_2.

In addition to the equilibrium state (3.8), conditions (3.7) and (3.4) reveal that another equilibrium state with, say, $dh_2=0$ is now possible, because in this case, $dK_2<0$. This new equilibrium state is denoted by $B_2^\dagger$ in Fig. 3. It is characterized by

$$h_1(B_2^\dagger)=h_1(B_1)+dh\dagger, h_2(B_2^\dagger)=h_2(B_1)=h_1(B_1),$$
$$dh\dagger>0, dh_2^\dagger=0, dK_1=0, dK_2<0, K_1(B_2^\dagger)=K_c, K_2(B_2^\dagger)<K_c. \tag{3.9}$$

Both states, B_2 and $B_2^\dagger$, which correspond to the same value of the load parameter, $\delta=\delta(B_1)+d\delta_0$, are stable; here, $d\delta_0$ is a fixed load increment. But as we shall show below, state $B_2^\dagger$ on the bifurcated path corresponds to a smaller stored elastic energy, and therefore is more stable.†

To this end we observe that *if there are no cracks* in the solid, the total stored elastic energy per unit cell (and per unit thickness in the direction normal to Fig. 1) is a finite quantity *proportional* to the thickness of the thermal layer, δ. This is because the temperature profiles (2.1) and (2.2) involve only y/δ and therefore integration of the elastic energy density over a unit cell would always lead to a quantity of the following kind:

$$\mathscr{E}(\delta)=A\delta, \tag{3.10}$$

where A is independent of δ, but depends on material parameters, total temperature drop, and the shape of the temperature profile. For profile (2.1), for example, we have (in plane strain, with the free surface‡)

$$A=\frac{19}{48}\frac{\hat{\alpha}^2T_0^2Eb}{(1-\nu)}, \tag{3.11}$$

and if we approximate the temperature profile (2.2) by $T=T_0[1-(1-y/\delta)^2]$, then we obtain

$$A=\frac{1}{10}\frac{\hat{\alpha}^2T_0^2Eb}{(1-\nu)}. \tag{3.12}$$

It is clear that in the present context other reasonable temperature profiles would always lead to

†The fact that the state with smaller stored elastic energy is more stable follows from Gibbs' statement of second law of thermodynamic; for the application of this to fracture problems, see Nemat-Nasser[12, 13].

‡Without the free surface, $(1-\nu)$ must be replaced with $(1-2\nu)$. δ is then measured from the center, along the crack.

an expression similar to (3.10), with A depending on the shape of the temperature profile, but not on δ.

When cracks exist, part of the total elastic energy given by (3.10) is used to generate crack surfaces, and the remaining part is stored in the body,

$$\mathscr{E} = \mathscr{E}_s + S, \tag{3.13}$$

where $\mathscr{E}_s$ is the stored elastic energy per unit cell and S is the corresponding surface energy. Since for a fixed δ the total supplied energy $\mathscr{E}$ is fixed, the state with larger total surface energy will have smaller stored elastic energy. Therefore, to prove that state $B_2^\dagger$ is more stable than B_2, we shall show that $S(B_2^\dagger) > S(B_2)$. However, since

$$S(B_2) = S(B_1) + 2(\mathrm{d}h_1 + \mathrm{d}h_2)\gamma,\ \mathrm{d}h_1 = \mathrm{d}h_2,$$

$$S(B_2^\dagger) = S(B_1) + 2\mathrm{d}h^\dagger\gamma,\ \mathrm{d}h_2^\dagger = 0, \tag{3.14}$$

to prove our assertion, we need only show that

$$(\mathrm{d}h_1 + \mathrm{d}h_2) = 2\mathrm{d}h_1 > \mathrm{d}h^\dagger; \tag{3.15}$$

in (3.14) γ is surface energy per unit area and relates to the critical value of the stress intensity factor by $K_c^2 = 2\gamma E/(1-\nu^2)$, where ν is the Poisson ratio and E Young's modulus.

To prove (3.15), we recall that the load parameter at both states, B_2 and $B_2^\dagger$, has the value $\delta(B_2) = \delta(B_2^\dagger) = \delta(B_1) + \mathrm{d}\delta_0$, where $\mathrm{d}\delta_0$ is fixed. It then follows that

$$\frac{\partial K_1}{\partial \delta}\mathrm{d}\,\delta_0 = \frac{\partial K_2}{\partial \delta}\mathrm{d}\delta_0 \quad \text{at} \quad B_1. \tag{3.16}$$

for point B_2 on the fundamental path, $\mathrm{d}h_1 = \mathrm{d}h_2$ and we obtain from eqn (3.2),

$$\mathrm{d}h_1 = -\frac{\partial K_1}{\partial \delta}\mathrm{d}\delta_0 \Big/ \left(\frac{\partial K_1}{\partial h_1} + \frac{\partial K_1}{\partial h_2}\right). \tag{3.17}$$

For point $B_2^\dagger$, on the other hand, $\mathrm{d}h_2^\dagger = 0$. Equations (3.2) then yield

$$\mathrm{d}h^\dagger = -\frac{\partial K_1}{\partial \delta}\mathrm{d}\delta_0 / \frac{\partial K_1}{\partial h_1}. \tag{3.18}$$

Now, in view of (3.7), we have $\mathrm{d}h^\dagger > 2\mathrm{d}h_1$ which is (3.15). Note that in expressions (3.16)–(3.18) the partial derivatives are all evaluated at state B_1, for which $h_1 = h_2$.

The fact that the state on the bifurcated path is more stable than the corresponding one on the fundamental path, may be proved in a different but equivalent manner. For this, one may consider two neighboring states and instead of fixing the load parameter, one chooses these two neighboring states in such a manner that *they correspond to the same total surface energy.* Then the state with smaller stored elastic energy would involve smaller total energy and therefore, would correspond to a smaller load parameter. Hence, it will be the one which actually will be attained. If the two neighboring states, $\hat{B}_2$ and $\hat{B}_2^\dagger$, one on the fundamental equilibrium path and the other on the bifurcated path, have the same surface energy, we must have, for the corresponding incremental crack lengths, $\mathrm{d}h_1 = \mathrm{d}h_2 = \frac{1}{2}\mathrm{d}h^\dagger$, and $\mathrm{d}h_2^\dagger = 0$. Then from (3.10) and (3.13) we obtain

$$\mathscr{E}_s(\hat{B}_2^\dagger) - \mathscr{E}_s(\hat{B}_2) = A\left[-2\left(\frac{\partial K_1}{\partial h_1}/\frac{\partial K_1}{\partial \delta}\right) + \left(\frac{\partial K_1}{\partial h_1} + \frac{\partial K_1}{\partial h_2}\right)/\frac{\partial K_1}{\partial \delta}\right]\mathrm{d}h_1 \tag{3.19}$$

which, in view of (3.7), yields

$$\mathscr{E}_s(\hat{B}_1^*) < \mathscr{E}_s(\hat{B}_2), \tag{3.20}$$

as required. Note that the actual states corresponding to a prescribed fixed load parameter may not be the same as those corresponding to a fixed surface energy.

To the second-order approximation used in arriving at (3.15), the two surface energies, one corresponding to a neighboring point on the fundamental path and the other to a point on the bifurcated path, would be equal at point B^*, i.e. we have

$$dh_1^* = 2dh_1 \text{ at } B^*. \tag{3.21}$$

However, if the higher-order terms are used, a conclusion similar to (3.15) will again be reached. We have circumvented the need for such a tedious consideration, by examining states in the neighborhood of point B_1 for which the strict inequality (3.7) holds; note that at point B^* conditions (3.5) hold.

3.3 *Post-critical response*

As discussed above, at the state corresponding to point B^*, every other crack in the array of cracks shown in Fig. 1 stops, as the remaining ones grow with increasing load parameter δ and at a rate initially twice as fast as before; this latter assertion follows from eqn (3.21). To examine the growth regime pattern after point B^*, we must consider three interacting cracks shown in Fig. 4, for which

$$h_1 = h_3, \quad h_2 = h_2(B^*) = \text{constant}, \quad K_1 = K_3 = K_c, K_2 < K_c. \tag{3.22}$$

However, since the spacing between cracks 1 and 3 in Fig. 4 is equal to $2b$, the corresponding initial interaction is weak. In fact, as it has been shown in [4], all the essential features of the crack growth regime after the bifurcation point can be established quantitatively with almost no loss in accuracy by considering only two interacting cracks for the present problem. Hence we shall pursue this approximation below.

On the bifurcated path $B^*B_1^*$ we have the following numerical results for temperature profile (2.1); for illustration we shall use this temperature profile:

$$dK_2 = \frac{\partial K_2}{\partial h_1} dh_1 + \frac{\partial K_2}{\partial \delta} d\delta < 0. \tag{3.23}$$

Hence, the stress intensity factor K_2 continues to decrease with increasing δ and h_1. At point B_1^* the stress intensity factor K_2 is zero, and a further increase in the load parameter results in the closure of crack 2. At this point and for temperature profile (2.1), calculations show that crack 2 snaps closed while crack 1 snaps into a finitely longer length, for infinitesimally larger values of the load parameter δ; this is illustrated in the next section. Hence point B_1^* defines a

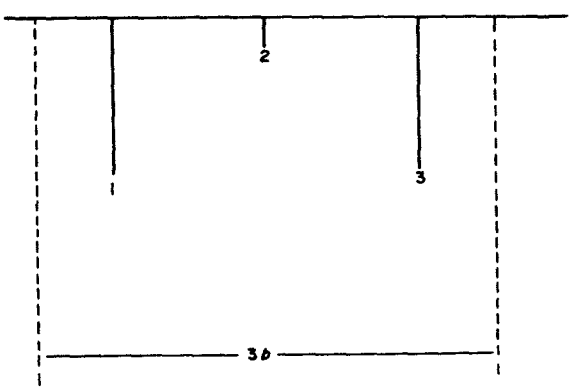

Fig. 4. A. unit cell with three unequal cracks: Crack 2 will involve both Model I and II.

snap-through critical state. In the infinitesimally small neighborhood of this state, there are no equilibrium states corresponding to (infinitesimal) $d\delta > 0$.

From the relation between the energy release rate and the stress intensity factor in Mode I, it has been shown in [3] that

$$K_1 \frac{\partial K_1}{\partial h_2} = K_2 \frac{\partial K_2}{\partial h_1}. \tag{3.24}$$

Since at point B_1^* we have $K_2 = 0$, this point is characterized by

$$\frac{\partial K_1}{\partial h_2} = 0. \tag{3.25}$$

Actually, since $\partial K_1/\partial h_2$ is in general non-positive, if this quantity is plotted as a function of h_1, the curve would be tangent to the h_1-axis at the critical point defined by (3.25); see Nemat-Nasser *et al.* [3].

For some other temperature profiles, e.g. (2.2), it happens that K_2 never reaches zero. In this case, crack 1 and 3 of Fig. 4 begin to have significant interaction, and one of them stops at a certain stable bifurcation point before the stress intensity factor at crack 2 can reach zero value. For cases of this kind there is no crack closure. This has been illustrated in [3] for temperature profile (2.2).

3.4 *Effect of small imperfections*

In the preceding discussions we consider idealized cases where the cracks are equally spaced and the material properties are homogeneous. This cannot exist in actual situations and there are always some imperfections present. It is known in structural analysis that even very small imperfections may introduce substantial reduction in the critical value of the load parameter at which the structure becomes unstable. It turns out that a similar role is played by small imperfections in the stability of a system of interacting tension cracks. The imperfection in the present case may be a small deviation from an equally spaced crack pattern (i.e. unequal crack spacing), or it may be small nonhomogeneity in material properties, e.g. the critical value or the stress intensity factor at one crack may exceed by a small amount that at the other crack in the unit cell of Fig. 2.

When the cracks are unequally spaced, then both Modes I and II will be involved and this will complicate the calculations substantially. On the other hand, when equal spacing is used, but different values are assigned to the critical stress intensity factor at the two cracks within a unit cell, the effect of imperfection can be studied without additional elaborate computations. For the purpose of illustration we shall give numerical examples in Section 4, using the latter type of imperfection.

To discuss the effect of imperfection, it is convenient to introduce the notation

$$u = h_1 - h_2$$

which measures deviation from the fundamental equilibrium path. Hence, in the u, δ-plane the fundamental equilibrium path coincides with the δ-axis; see Fig. 5(a). At point B^*, condition (3.5) is first satisfied, and hence, this is a stable bifurcation point. At point B_u, critical condition (2.6) holds, and hence, this is an unstable bifurcation point. All points above B_u on the δ-axis in Fig. 5(a) are unstable bifurcation points; at these points, the bifurcated equilibrium path has a negative slope, the slope being zero at B_u. All points on the δ-axis between B^* and B_U are stable bifurcation points.

The path $B^*B_1^*$ in the u, δ-plane is the bifurcated path on which $h_2 = h_2(B^*) = \text{constant}$, $K_2 < K_c$, and, as we discussed before, this is the path that actually will be followed in the absence of any imperfection.

Assume now that the critical stress intensity factor at crack 1 is K_c, but that at crack 2 is $K_c + \varepsilon K_c$, where $\varepsilon \ll 1$, e.g. ε = few percent. Then, as δ is increased, crack 2 will have a shorter length than crack 1 (see Fig. 5b), and therefore, u as a function of δ will follow a path similar

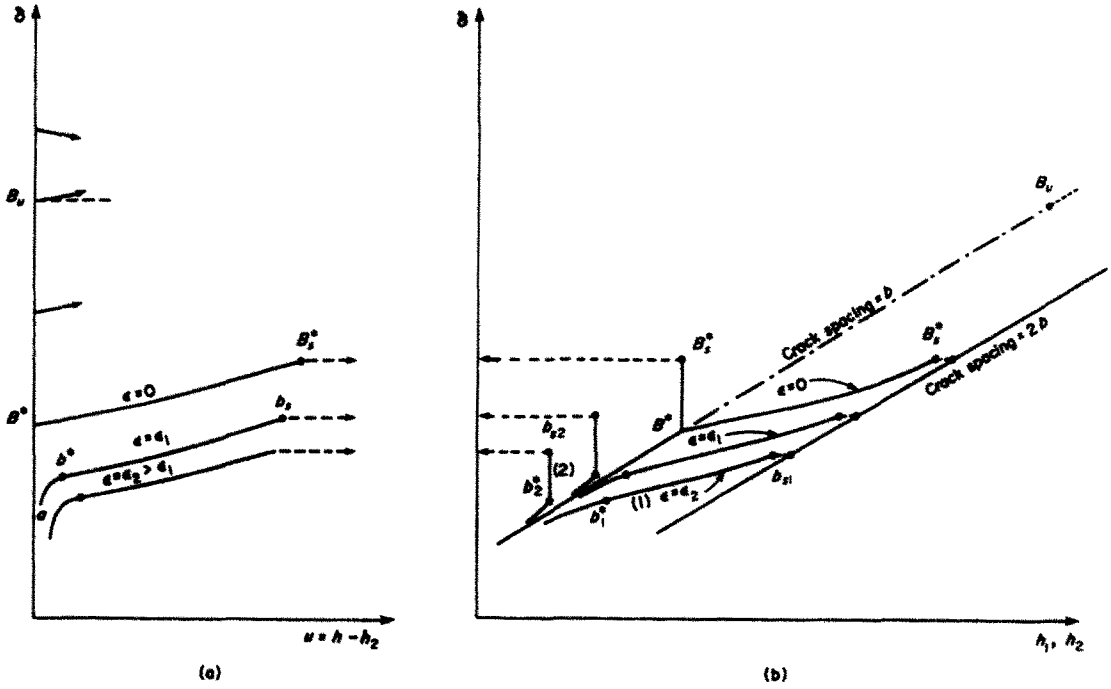

Fig. 5. Post-critical response and the effect of imperfection.

to that sketched in Fig. 5(a) by curve ab_s. At a certain point, say, b^* (Fig. 5a), on this curve, crack 2 stops growing, and crack 1 then continues to grow at a faster rate; the corresponding point, on curve 1 is denoted by b_1^* and that on curve 2 by b_2^* in Fig. 5(b). For a certain temperature profile, e.g. (2.1), the stress intensity factor at crack 2 reaches zero at point b_s in Fig. 5(a), after which crack 2 snaps closed as crack 1 extends by a finite amount. At this point, u increases by a large finite value. The crack spacing is then doubled, and the whole process repeats itself.

To give an analytic description of some of the above behaviors, one may use a perturbation approach as follows.

The crack lengths for nonzero ε are functions of this parameter, $h_i = h_i(\varepsilon)$, $i = 1, 2$, so are the stress intensity factors $K_i = K_i(h_1, h_2; \delta, \varepsilon)$. Hence, for *fixed* δ we may write

$$h_1(\varepsilon) = h_1(0) + \Delta h_1, \quad h_2(\varepsilon) = h_2(0) + \Delta h_2, \tag{3.26}$$

and

$$K_1(\varepsilon) = K_c + \frac{\partial K_1}{\partial h_1}\Delta h_1 + \frac{\partial K_1}{\partial h_2}\Delta h_2 = K_c,$$

$$K_2(\varepsilon) = K_c + \frac{\partial K_2}{\partial h_1}\Delta h_1 + \frac{\partial K_2}{\partial h_2}\Delta h_2 = K_c + \varepsilon K_c, \tag{3.27}$$

where on the fundamental path, $h_1(0) = h_2(0)$ and $K_1 = K_2 = K_c$. In eqns (3.26) and (3.27) all partial derivatives are evaluated on the fundamental equilibrium path, i.e. at $\varepsilon = 0$. Furthermore, it is assumed that the deviations from the fundamental path, denoted by Δh_1 and Δh_2, are small; eqns (3.27) apply to points below critical point b^* in Fig. 5(a).

Equations (3.27) can be solved for Δh_1 and Δh_2, and since on the fundamental equilibrium path $\partial K_1/\partial h_1 = \partial K_2/\partial h_2 < 0$ and $\partial K_1/\partial h_2 = \partial K_2/\partial h_1 < 0$, we obtain

$$\Delta h_1 \simeq -\left[K_c \frac{\partial K_1}{\partial h_2} \Big/ \left\{\left(\frac{\partial K_1}{\partial h_1}\right)^2 - \left(\frac{\partial K_1}{\partial h_2}\right)^2\right\}\right]\varepsilon > 0,$$

$$\Delta h_2 \simeq \left[K_c \frac{\partial K_1}{\partial h_1} \Big/ \left\{\left(\frac{\partial K_1}{\partial h_1}\right)^2 - \left(\frac{\partial K_1}{\partial h_2}\right)^2\right\}\right]\varepsilon < 0, \tag{3.28}$$

where, since the derivatives in (3.28) are calculated below the stable bifurcation point B^* of Fig. 3, conditions (3.1) are valid and hence,

$$D \equiv \left(\frac{\partial K_1}{\partial h_1}\right)^2 - \left(\frac{\partial K_1}{\partial h_2}\right)^2 > 0. \tag{3.29}$$

As long as D is a relatively large finite quantity, $|\Delta h_i|$ remains of the order of ε, as shown by (3.28). As we increase δ, the positive quantity D tends to decrease, becoming zero at the stable bifurcation point B^*. Hence, the deviation from the fundamental equilibrium path, characterized by

$$\begin{aligned} u &= h_1(\varepsilon) - h_2(\varepsilon) = \Delta h_1 - \Delta h_2 \\ &\simeq -\varepsilon K_c \left[\frac{\partial K_1}{\partial h_1} + \frac{\partial K_1}{\partial h_2}\right] / D \\ &= \varepsilon K_c / \left(\frac{\partial K_1}{\partial h_2} - \frac{\partial K_1}{\partial h_1}\right), \end{aligned} \tag{3.30}$$

tends to increase with increasing δ; approximation (3.30) is valid only for points below the critical point b^* in Fig. 5(a) which correspond to points $b\frac{\dagger}{2}$ and $b\frac{\ddagger}{2}$ in Fig. 5(b).

For a fixed value of imperfection, $\varepsilon = \varepsilon_0$ and for $\delta < \delta^*$, consider an increment in the load parameter, $\mathrm{d}\delta > 0$, and calculate the corresponding increase in crack lengths, $\mathrm{d}h_1$ on curve (1) and $\mathrm{d}h_2$ on curve (2), of Fig. 5(b). Since the new state must be in equilibrium, we have

$$\begin{aligned} \frac{\partial K_1}{\partial h_1}\mathrm{d}h_1 + \frac{\partial K_1}{\partial h_2}\mathrm{d}h_2 + \frac{\partial K_1}{\partial \delta}\mathrm{d}\delta = 0, \\ \frac{\partial K_2}{\partial h_1}\mathrm{d}h_1 + \frac{\partial K_2}{\partial h_2}\mathrm{d}h_2 + \frac{\partial K_2}{\partial \delta}\mathrm{d}\delta = 0, \end{aligned} \tag{3.31}$$

where the partial derivatives are calculated on curves (1) and (2). Note that, unlike the corresponding expressions in eqns (3.2), here $\partial K_1/\partial h_1 \neq \partial K_2/\partial h_2$, $\partial K_1/\partial h_2 \neq \partial K_2/\partial h_1$, and $\partial K_1/\partial \delta \neq \partial K_2 \partial \delta$. We now solve (3.31), and obtain

$$\frac{\mathrm{d}h_2}{\mathrm{d}h_1} = \left[\frac{\partial K_2}{\partial h_1}\frac{\partial K_1}{\partial \delta} - \frac{\partial K_1}{\partial h_1}\frac{\partial K_2}{\partial \delta}\right] \Big/ \left[\frac{\partial K_1}{\partial h_2}\frac{\partial K_2}{\partial \delta} - \frac{\partial K_2}{\partial h_2}\frac{\partial K_1}{\partial \delta}\right]. \tag{3.32}$$

At point $b\frac{\ddagger}{2}$, $\mathrm{d}h_2 = 0$ and hence, this state is characterized by

$$\frac{\partial K_2}{\partial h_1}\frac{\partial K_1}{\partial \delta} - \frac{\partial K_1}{\partial h_1}\frac{\partial K_2}{\partial \delta} = 0. \tag{3.33}$$

In the absence of imperfection, (3.33) reduces to the critical condition defined by (3.5).

Equation (3.24) remains valid provided that the quantites are evaluated at $\varepsilon = \varepsilon_0$, and for h_1 and h_2, given by the corresponding points on curves (1) and (2). Hence, (3,25) defines the snap-through critical point b_s in Fig. 5(a).

3.5 *Summary of basic results*

For the two interacting cracks shown in Fig. 2, the fundamental equilibrium path is defined by

$$h_1 = h_2, \quad K_1 = K_2 = K_c. \tag{3.34}$$

The fundamental equilibrium path will be followed as long as

$$\frac{\partial K_1}{\partial h_1} = \frac{\partial K_2}{\partial h_2} < \frac{\partial K_1}{\partial h_2} = \frac{\partial K_2}{\partial h_1} < 0. \tag{3.35}$$

The first critical point is a stable bifurcation point attained when

$$\frac{\partial K_1}{\partial h_1}=\frac{\partial K_2}{\partial h_2}=\frac{\partial K_1}{\partial h_2}=\frac{\partial K_2}{\partial h_1}<0. \tag{3.36}$$

All points on the fundamental equilibrium path for which

$$0>\frac{\partial K_1}{\partial h_1}=\frac{\partial K_2}{\partial h_2}>\frac{\partial K_1}{\partial h_2}=\frac{\partial K_2}{\partial h_1} \tag{3.37}$$

holds, are stable bifurcation points. The unstable bifurcation point is first reached when

$$\frac{\partial K_1}{\partial h_1}=\frac{\partial K_2}{\partial h_2}=0. \tag{3.38}$$

All points on the fundamental equilibrium path for which

$$\frac{\partial K_1}{\partial h_1}=\frac{\partial K_2}{\partial h_2}>0 \tag{3.39}$$

holds, are unstable bifurcation points. In all cases we always have on the fundamental equilibrium path,

$$\frac{\partial K_1}{\partial h_2}=\frac{\partial K_2}{\partial h_1}<0; \tag{3.40}$$

this has been proved elsewhere, [3]. On the bifurcated path, on the other hand, $K_1\neq K_2$ and, instead of (3.40), we have

$$K_1\frac{\partial K_1}{\partial h_2}=K_2\frac{\partial K_2}{\partial h_1}\leq 0, \tag{3.41}$$

the equality sign corresponding to the snap-through instability point at which, say, $K_2=0$ and hence, crack 2 snaps closed as crack 1 extends by a finite amount.

The introduction of a very small material imperfection results in deviation of the equilibrium path from the fundamental equilibrium path for all finite values of δ and this deviation increases with increasing δ. Along the new equilibrium paths, the crack with the larger value of the critical stress intensity factor, say crack 2, stops at the critical state defined by

$$\frac{\partial K_2}{\partial h_1}\frac{\partial K_1}{\partial \delta}-\frac{\partial K_1}{\partial h_1}\frac{\partial K_2}{\partial \delta}=0. \tag{3.42}$$

After this, crack 1 continues to grow with increasing δ, until the snap-through critical state defined by

$$\frac{\partial K_1}{\partial h_2}=0. \tag{3.43}$$

is reached. An infinitesimal increase in δ then results in a snap closure of crack 2, as crack 1 extends by a finite amount.

4. NUMERICAL RESULTS

In this section the theory is illustrated by means of numerical examples. Consider an infinite strip of finite width 2L, containing equally spaced edge cracks at both its edges; see Fig. 6. We shall examine the growth regime of these cracks for both temperature profiles (2.1) and (2.2). To associate our results with those presented in [3,4,11], we choose the critical value of the stress

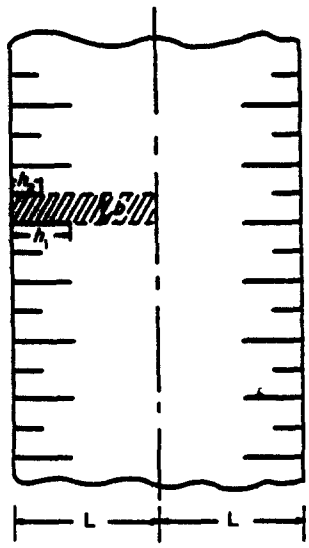

Fig. 6. A strip with periodically spaced edge cracks.

intensity factor at†

$$K_c = 0.06\hat{\beta}T_0\sqrt{2\pi L}, \quad \hat{\beta} = \hat{\alpha}E/(1-\nu), \tag{4.1}$$

and introduce the following non-dimensional quantities:

$$C_m = h_m/L, F_m = K_m/\hat{\beta}T_0\sqrt{\pi L},$$
$$\frac{\partial F_m}{\partial C_n} = \left(\frac{\partial K_m}{\partial h_n}\right)/\hat{\beta}T_0\sqrt{\pi L}, \quad m,n = 1,2. \tag{4.2}$$

4.1 *Temperature profile* (2.1)

To obtain the fundamental equilibrium path, we choose (arbitrarily) the initial crack spacing such that $b/L = 0.16$. Then for each value of the load parameter δ, we calculate $h_1 = h_2$ such that $K_1 = K_2 = K_c$. In Fig. 7 curve AB is obtained in this manner. For states corresponding to the AB^* portion of this path, $\partial F_1/\partial C_1 = \partial F_2/\partial C_2 \leq \partial F_1/\partial C_2 = \partial F_2/\partial C_1 < 0$, the equality sign corresponding to the stable bifurcation point B^*. Although states between B^* and B_u on this path are stable, another stable equilibrium path emanates form each of these points. Correct to about 1%, the stable bifurcation point B^* is defined by $\delta/L = 0.315$ and $C_1 = C_2 = 0.274$; this crack length is less than half of the crack length pertaining to the unstable critical point B_u obtained in [3, 11].

After point B^*, crack 2 ceases to grow, while crack 1 continues to extend, as δ is increased. As is shown in Fig. 7 the growth rate is initially twice as fast as that on the fundamental equilibrium path.

This leads to the stable branch $B^*B_s^*$ on which $\partial F_1/\partial C_1 < 0$. Along this branch, F_2, as well as $|\partial F_1/\partial C_2|$, continue to decrease monotonically with increasing δ, as shown in Fig. 8, attaining zero when $\delta/L = 0.420$ and $C_1 = 0.387$. At this point, The changes in the stress intensity factors are given by

$$dF_1 = -1.571\,dC_1 - 0.007\,dC_2 + 1.596\,d(\delta/L),$$
$$dF_2 = -0.173\,dC_1 + 0.956\,dC_2 - 0.645\,d(\delta/L). \tag{4.3}$$

Since $F_1 = K_c/\hat{\beta}T_0\sqrt{\pi L}$, and $F_2 = 0$ at this point, the only admissible change is such that $dF_1 < 0$

†In [3,4], $\hat{\beta}$ has been *incorrectly* given as $3\hat{\alpha}E/(1-2\nu)$. The results which are all in dimensionless form, are *not* however, affected by this.

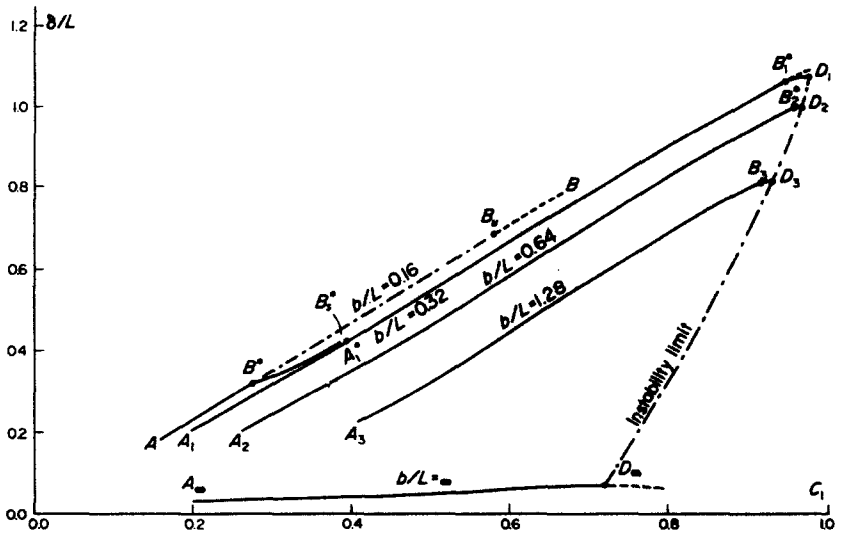

Fig. 7. δ,h_1-space temperature profile eqn (2.1).

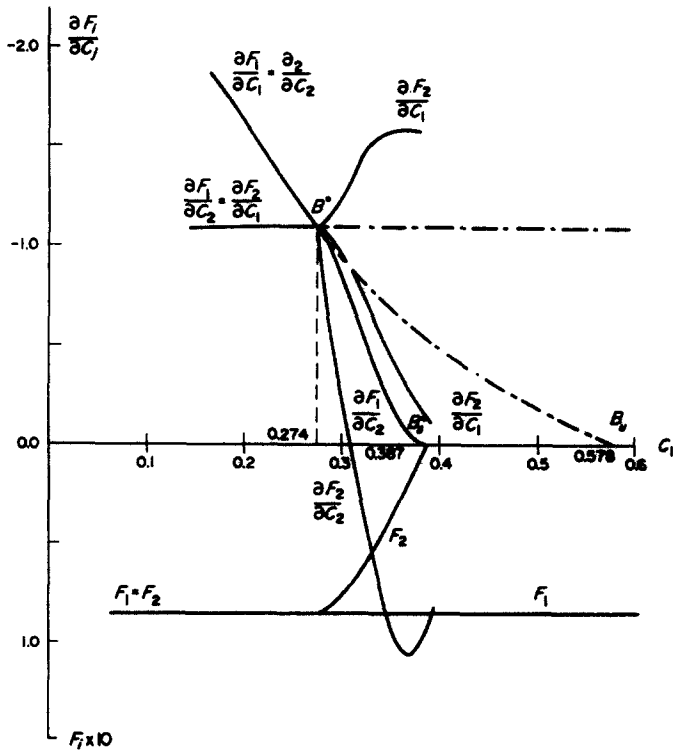

Fig. 8. Stress intensity factors and their derivatives with respect to crack lengths; $b/L = 0.16$.

and $dF_2 = 0$. These relations imply

$$d(\delta/L) < 0, \quad dC_1 = 0, \quad dC_2 = 0.674\,d(\delta/L) < 0. \tag{4.4}$$

Hence we have a snap-through critical state at which crack 2 closes and crack 1 extends by a small but finite amount. The crack spacing is then doubled, $b/L = 0.32$.

Branch $A\dagger B\dagger$ in Fig. 7 corresponds to the state in which every other crack is closed. This new state is stable, since $\partial F_1/\partial C_1 = \partial F_2/\partial C_2 < \partial F_1/\partial C_2 = \partial F_2/\partial C_1 < 0$. A stable bifurcation occurs at the point $B\dagger$ where $\delta L = 1.064$ and $C_1 = C_2 = 0.946$. After this point, crack 2 ceases to grow and a process similar to that described above may be expected. However, since the strip has a finite

width, another critical point, D_1, will be attained, where $\delta/L = 1.077$, $C_1 = 0.977$, and $\partial F_1/\partial C_1 = d\delta/dh_1 = 0$. The final fracture of the strip occurs at D_1, where cracks from the opposite sides of the strip join spontaneously. If the initial crack spacing is larger than $b/L = 0.32$, then one stable bifurcation point with the consequent fracture of the strip is encountered. Numerical results for $b/L = 0.64$ and 1.28 are also shown in Fig. 7. As an extreme case the results for $b/L = \infty$ is calculated by the simple integration given in Appendix C. In this case, the stable bifurcation point B^* does not exist, and the critical point D_∞ corresponds to $\delta/L = 0.065$ and $C_1 = 0.72$.

Consider now the effect of small imperfections. To this end let the critical value of the stress intensity factor at crack 1 be given by (4.1) and that at crack 2 by $K_C + \varepsilon K_C$. For $\varepsilon = 0.03$ and 0.09 the corresponding crack growth regimes are shown in Fig. 9. Crack 1 which has a smaller critical value of the stress intensity factor, grows at a faster rate than crack 2. Crack 2 stops at point b^*, while crack 1 continues to grow with increasing δ, until point b_s^* at which it snaps into the new branch A_1B_1, while crack 2 snaps closed. For $\varepsilon = 0.03$ we have $\delta(b^*)/L = 0.238$, $h_1(b^*)/L = 0.214$ and $h_2(b^*)/L = 0.200$, whereas for $\varepsilon = 0.09$ the corresponding quantities are 0.193, 0.177 and 0.160. The snap-through occurs for $\varepsilon = 0.03$ at $\delta(b_s)/L = 0.324$, $h_1(b_s)/L = 0.306$ and for $\varepsilon = 0.09$ at respective values of 0.274 and 0.261.

4.2 *Temperature profile* (2.2)

For this temperature profile the results are given in Fig. 10. Curves AB and A_1B_1 are the fundamental paths for $b/L = 0.32$ and 0.64, respectively. On these curves B^* and $B\dagger$ are the corresponding stable bifurcation points. At B^* crack 2 stops, while crack 1 grows at a faster rate, forming a bifurcated path which approaches the second fundamental path A_1B_1 close to the latter's stable bifurcation point $B\dagger$. In this case, however, no crack closure occurs. In [4] it has been shown that even if three interacting cracks are considered, Fig. 4, still no crack closure is predicted and while the stress intensity factor at crack 2 is still finite, cracks 1 and 3

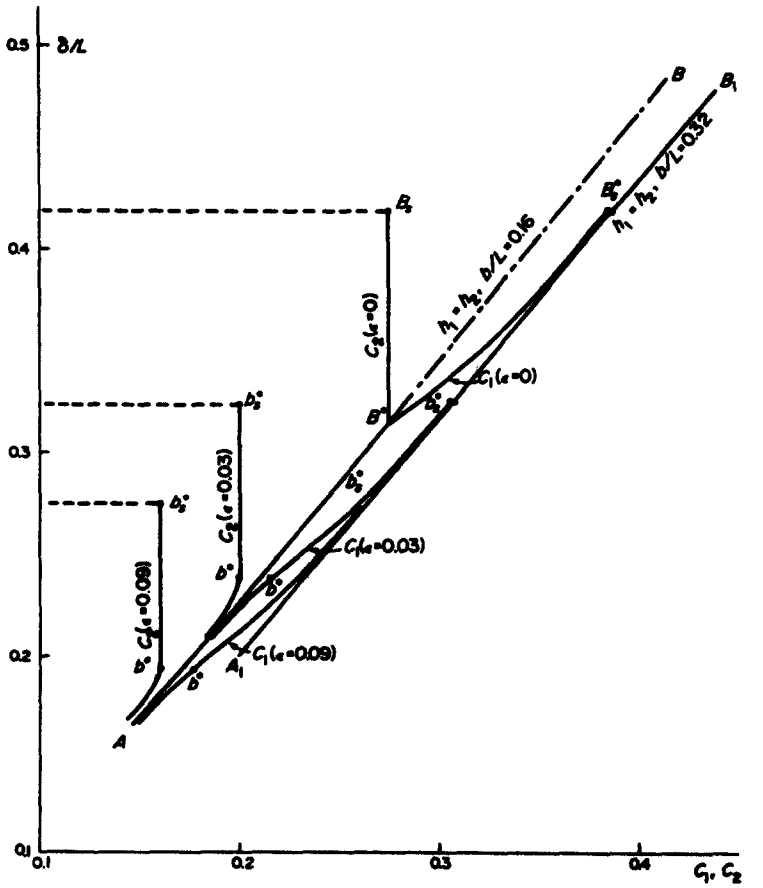

Fig. 9. Crack growth regime for two interacting cracks in a unit cell; temperature profile eqn (2.1).

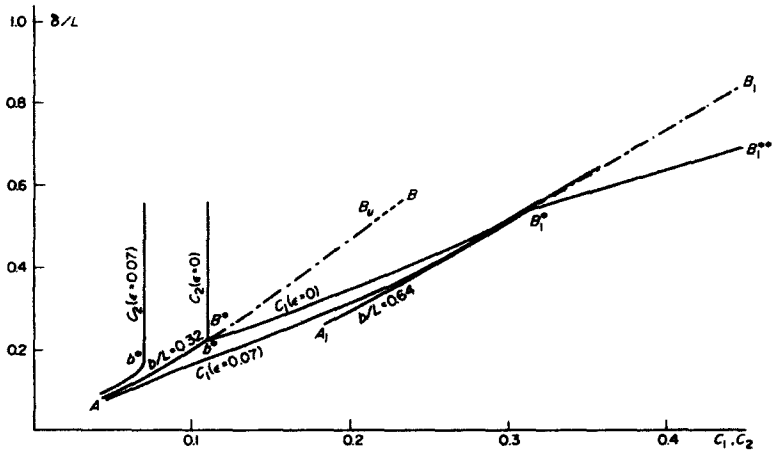

Fig. 10. Crack growth regime for two interacting cracks in a unit cell; temperature profile eqn (2.2).

become highly interactive and in fact, one of them stops growing as the other continues to grow at a faster rate; see [4] for further discussion.

We have also examined the effect of initial imperfection in the crack growth regime for temperature profile (2.2). Figure 10 shows the results for $\varepsilon = 0.07$. In this figure, $\delta(b^*)/L = 0.168$, $h_1(b^*)/L = 0.102$ and $h_2(b^*)/L = 0.070$. Note that $\delta(b^*)/L$ is more than 25% smaller than $\delta(B^*)/L = 0.221$.

Acknowledgements—This work was supported by the National Science Foundation under Grant ENG 77-22155 and by the Los Alamos Scientific Laboratory, University of California, under contract P.O. No. N68-8539G-1 to Northwestern University.

REFERENCES

1. S. Nemat-Nasser, Overview of the basic progress in Ductile fracture, (Invited Lecture). *Transactions 4th int. Conf. on Structural Mechanics in Reactor Technology*, (Edited by T. A. Jaeger and B. A. Boley), Vol. L Inelastic Analysis of Metal Structures, paper L2/1, (see Sec. 5) (1977).
2. S. Nemat-Nasser, Stability of system of interacting cracks. *Letters in Appl. Engng and Science* 16, 277–285 (1978).
3. S. Nemat-Nasser, L. M. Keer and K. S. Parihar, Unstable growth of thermally induced interacting cracks in brittle solids. *Int. J. Solids Structures* 14, 409–430 (1978).
4. L. M. Keer, S. Nemat-Nasser and A. Oranratnachai, Unstable growth of thermally induced interacting cracks in brittle solids: further results *Int. J. Solids Structures* 15, 111–126 (1979).
5. L. M. Keer, S. Nemat-Nasser and K. S. Parihar, Growth and stability of thermally induced interacting cracks in brittle solids. *Geothermal Energy Research Report*, Northwestern University, (Sept. 1976).
6. T. Von Karman and H. S. Tsien, The buckling of spherical shells by external pressure. *J. Aero. Sci.* 7, 43–50 (1939).
7. J. W. Hutchinson and W. T. Koiter, Postbuckling theory. *Appl. Mech. Reviews* 23, 1353–1366 (1970).
8. A. H. Chilver, The elastic stability of structures. In *Stability* (Edited by H. Leipholz), Chap. 3. University of Waterloo, Waterloo, Ontario (1972).
9. J. Roorda, Concepts in elastic structural stability. In *Mechanics Today* (Edited by S. Nemat-Nasser), Vol. 1, Chap. 7, pp. 322–372. Pergamon Press (1974).
10. S. Nemat-Nasser, Geothermal energy: extracting heat from hot dry rock masses. *Proc. of the 16th Midwestern Mechanics Conf.*, pp. 285–297. Kansas State University, (Sept. 19–21, 1979).
11. Y. Sumi, S. Nemat-Nasser and L. M. Keer, A new combined analytical and finite-element solution method for stability analysis of the growth of interacting tension cracks in brittle solids *Earthquake Engineering and Research Laboratory, Technical Report No.* 79-5-14, Dept. Civil Engineering, Northwestern University, Evanston, Ill., (May 1979); *Int. J. Engng Sci.* 18, 211–224 (1980).
12. S. Nemat-Nasser, Variational methods for analysis of stability of interacting cracks. *Proc. of the IUTAM Symposium on Variational Methods in the Mechanics of Solids*, Evanston, Ill. (11–13 Sept. 1978) (Edited by S. Nemat-Nasser). Pergamon Press, New York.
13. S. Nemat-Nasser, The second law of thermodynamics and noncollinear crack Growth. In *Proc. of the Third AS CE/EMD Specialty Conference*, pp. 449–452. Austin, Texas (17–19 Sept. 1979).
14. Y. Yamamoto, Finite element approaches with the aid of analytical solutions. *Recent Advances in Matrix Methods of Structual Analysis and Design*, 85–103, Univ. Alabama Press (1971).
15. Y. Yamamoto and N. Tokuda, Determination of stress intensity factors in cracked plates by the finite element method. *Int. J. Numer. Meth. in Engng* 6, 427–439 (1973).
16. H. Tada, *Handbook of Stress Intensity Factors*, Del Research Cooperation (1973).

APPENDIX A

Method of analysis

Let V denote the region occupied by the elastic body. In the absence of body forces, the field equations are,

$$\sigma_{ij,j} = 0 \text{ in } V,$$
$$\sigma_{ij}n_j = t_i \text{ on } S_t, \tag{A.1}$$
$$u_i = \bar{u}_i \text{ on } S_u,$$

where comma followed by an index denotes partial differentiation with respect to the corresponding cordinate, the summation convention on repeated indices is used and n_j denotes the components of the exterior unit normal to the boundary of the solids; S_t is the part of the boundary on which some components of tractions, t_i, are prescribed and S_u is part on which some components of the displacement, $\bar{u}_i$, are given. The unit cell and the corresponding elasticity boundary value problem is shown in Fig. A1. The equivalent thermal tractions are

$$t_1(x_1, -b/2) = 0,$$
$$t_2(x_1, -b/2) = -\hat{\beta}(T - T_0), 0 \le x_1 \le h_1; \tag{A.2}$$

$$t_1(x_1, b/2) = 0,$$
$$t_2(x_1, b/2) = \hat{\beta}(T - T_0), 0 \le x_1 \le h_2; \tag{A.3}$$

where $\hat{\beta} = \hat{\alpha}E/(1-\nu)$, $\hat{\alpha}$ being the coefficient of thermal expansion.†

According to[11], we first determine the relation between crack lengths (h_1, h_2) and the penetration depth δ/L in such a manner that the stress intensity factors of each growing crack maintain its critical value. Then we calculate the derivatives of the stress intensity factors, $\partial K_m/\partial h_n$, for the purpose of stability analysis.

The dominant terms of stresses around the mth crack tip can be represented in the following form:

$$\sigma_{ij}^{(m)} = a_1^{(m)}\sigma_{ij}^1(r_m, \theta_m) + a_2^{(m)}\sigma_{ij}^2(r_m, \theta_m) + b_1^{(m)}\bar{\sigma}_{ij}^1(r_m, \theta_m) + b_2^{(m)}\bar{\sigma}_{ij}^2(r_m, \theta_m) + 0(r_m^{3/2}), \tag{A.4}$$

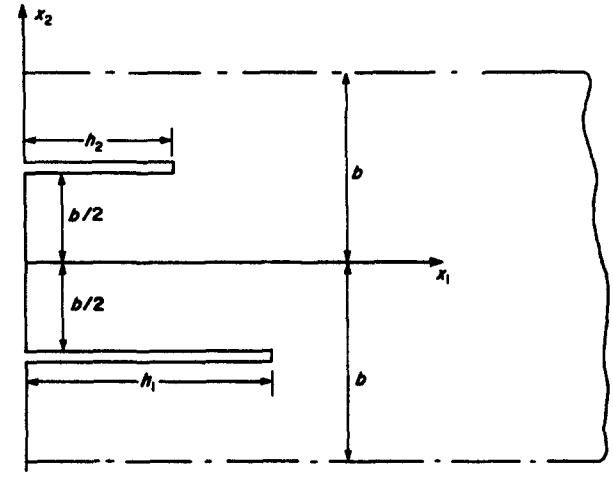

(a)

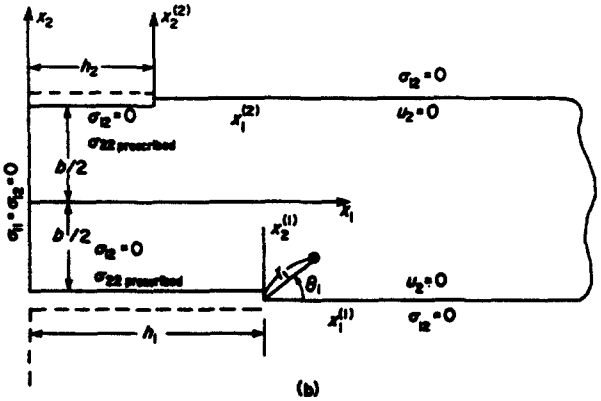

(b)

Fig. A1. (a) Typical unit cell consisting of two interacting edge cracks; (b) The basic elasticity boundary-value problem.

†In[3, 4], $\hat{\beta}$ has been *incorrectly* given as $3\hat{\alpha}E/(1-2\nu)$. The results which are all in dimensionless form, are *not* however, affected by this.

where (r_m, θ_m) is a local polar coordinate whose origin is located at the mth crack tip and $\sigma_{ij}^k(r_m, \theta_m)$ and $\tilde{\sigma}_{ij}^k(r_m, \theta_m)$, $k = 1,2$, are given in Appendix B. The coefficients $b_1^{(m)}$ and $b_2^{(m)}$ can easily be determined as the Taylor expansion coefficients of applied tractions at the mth crack tip, while $a_1^{(m)}$ and $a_2^{(m)}$ are determined by the method of superposition of analytical and finite-element solutions [11,14,15]. The stress intensity factor K_m is expressed as

$$K_m = \frac{3\sqrt{2\pi}}{4} a_1^{(m)}, \tag{A.5}$$

and the load parameter δ is so determined that K_m equals the critical value at the growing crack tip.

If we differentiate eqn (A.1) with respect to the crack length h_n, the solution of the problem, $\partial\sigma_{ij}/\partial h_n$, is obtained as

$$\frac{\partial \sigma_{ij}^{(m)}}{\partial h_n} = \begin{cases} -\frac{3}{2} a_1^{(n)} \sigma_{ij}^0 + \left(\frac{\partial a_1^{(n)}}{\partial h_n} - \frac{5}{2} a_2^{(n)}\right) \sigma_{ij}^1 + \left(\frac{\partial b_1^{(n)}}{\partial h_n} - 3 b_2^{(n)}\right) \tilde{\sigma}_{ij}^1 + 0(r_m^{1/2}) & \text{for } m = n, \\ \frac{\partial a_1^{(m)}}{\partial h_n} \sigma_{ij}^1 + \frac{\partial b_1^{(m)}}{\partial h_n} \tilde{\sigma}_{ij}^1 + 0(r_m^{1/2}) & \text{for } m \neq n, \end{cases} \tag{A.6}$$

near the mth crack tip, where σ_{ij}^0 has a singularity of $0(r_m^{-3/2})$ as shown in Appendix B. Here we define new variables,

$$\sigma_{nij} = \frac{\partial \sigma_{ij}}{\partial h_n} + \frac{3}{2} a_1^{(n)} \sigma_{ij}^0,$$

$$u_{ni} = \frac{\partial u_i}{\partial h_n} + \frac{3}{2} a_1^{(n)} u_i^0, \; n = 1,2, \tag{A.7}$$

where u_i^0 represents the displacement field corresponding to the stress field σ_{ij}^0. These variables are chosen in such a manner that the singularity of the order $r_n^{-3/2}$ is removed from the derivative problem. With the aid of (A.7), and upon differentiation of (A.1) with respect to h_n, we write

$$\sigma_{nij,j} - \frac{3}{2} a_1^{(n)} \sigma_{ij,j}^0 = 0 \quad \text{in } V,$$

$$\sigma_{nij} n_j = \frac{\partial t_i}{\partial h_n} + \frac{3}{2} a_1^{(n)} \sigma_{ij}^0 n_j \quad \text{on } S_t,$$

$$u_{ni} = \frac{\partial \bar{u}_i}{\partial h_n} + \frac{3}{2} a_1^{(n)} u_1^0 \quad \text{on } S_u, \; n = 1,2. \tag{A.8}$$

The stress distribution around the mth crack tip can be expressed in the same manner as (A.4); here, this becomes

$$\sigma_{nij}^{(m)} = \alpha_{n1}^{(m)} \sigma_{ij}^1(r_m, \theta_m) + \alpha_{n2}^{(m)} \sigma_{ij}^2(r_m, \theta_m) + \left(\frac{\partial b_1^{(m)}}{\partial h_n} - 3 b_2^{(m)}\right) \tilde{\sigma}_{ij}^1 + 0(r_m). \tag{A.9}$$

The unknown coefficients $\alpha_{nk}^{(m)}$, $k, m, n = 1, 2$, can be determined by the same method used for the analysis of stress intensity factors. Comparing (A.6) and (A.9), the derivatives of the stress intensity factors are obtained as

$$\frac{\partial K}{\partial h_n} = \begin{cases} \frac{3\sqrt{2\pi}}{4} \left(\alpha_{n1}^{(n)} + \frac{5}{2} a_2^{(n)}\right) & \text{for } m = n, \\ \frac{3\sqrt{2\pi}}{4} \alpha_{n1}^{(m)} & \text{for } m \neq n. \end{cases} \tag{A.10}$$

APPENDIX B

Various stress fields used in Appendix A, are summarized below.

$$\sigma_{ij}^0 = -\tfrac{1}{8} r_m^{-3/2} \begin{cases} 2\cos(\theta_m/2) - 3\sin\theta_m \sin(5\theta_m/2), & i = j = 1, \\ 2\cos(\theta_m/2) + 3\sin\theta_m \sin(5\theta_m/2), & i = j = 2, \\ 3\sin\theta_m \cos(5\theta_m/2), & i = 1, j = 2; \quad i = 2, j = 1. \end{cases} \tag{B.1}$$

$$\sigma_{ij}^1 = \tfrac{3}{4} r_m^{-1/2} \cos(\theta_m/2) \begin{cases} 1 - \sin(\theta_m/2)\sin(3\theta_m/2), & i = j = 1, \\ 1 + \sin(\theta_m/2)\sin(3\theta_m/2) & , i = j = 2, \\ \sin(\theta_m/2)\cos(3\theta_m/2), & i = 1, j = 2; i = 2, j = 1. \end{cases} \tag{B.2}$$

$$\sigma_{ij}^2 = \tfrac{1}{4} r_m^{1/2} \cos(\theta_m/2) \begin{cases} 1 + \sin^2(\theta_m/2), & i = j = 1, \\ 1 - \sin^2(\theta_m/2), & i = j = 2, \\ -\sin(\theta_m/2)\cos(\theta_m/2), & i = 1, \quad j = 2; i = 2, j = 1. \end{cases} \tag{B.3}$$

$$\tilde{\sigma}_{ij}^1(r_m, \theta_m) = \begin{cases} 2 + \text{constant}, & i = j = 1, \\ 2, & i = j = 2, \\ 0, & i \neq j. \end{cases} \tag{B.4}$$

$$\tilde{\sigma}_{ij}^2(r_m, \theta_m) = \begin{cases} 5 r_m \cos\theta_m, & i = j = 1, \\ 6 r_m \cos\theta_m, & i = j = 2, \\ -6 r_m \sin\theta_m, & i \neq j. \end{cases} \tag{B.5}$$

APPENDIX C

Symmetric edge cracks in a strip

According to Tada[16], the stress intensity factor of the cracks shown in Fig. C1 can be expressed as

$$K = \sqrt{2\tan\left(\frac{\pi h}{2L}\right)/L}\int_0^h P(\xi)\left\{1+f(\xi/h)\cos^2\left(\frac{\pi h}{2L}\right)\right\}\frac{d\xi}{\left[1-\left\{\cos\left(\frac{\pi h}{2L}\right)/\cos\left(\frac{\pi\xi}{2L}\right)\right\}^2\right]^{1/2}} \tag{C.1}$$

where

$$P(\xi) = \beta T_0\begin{cases}1.0 & \text{for } 0 \le \xi \le \delta/(n+1),\\ \frac{1}{2}\left\{1.0+\cos\pi\left(\frac{\xi(n+1)-\delta}{n\delta}\right)\right\} & \text{for } \delta/(n+1) \le \xi \le \delta,\\ 0.0 & \text{for } \xi > \delta,\end{cases} \tag{C.2}$$

and

$$f(\xi/h) = 1.30 - 0.69(\xi/h)^2 + 0.39(\xi/h)^3. \tag{C.3}$$

Numerical calculations are performed to obtain the relations between crack length h and the penetration depth δ, such that $K = K_c$ at the crack tip and the results are shown in Fig. 7.

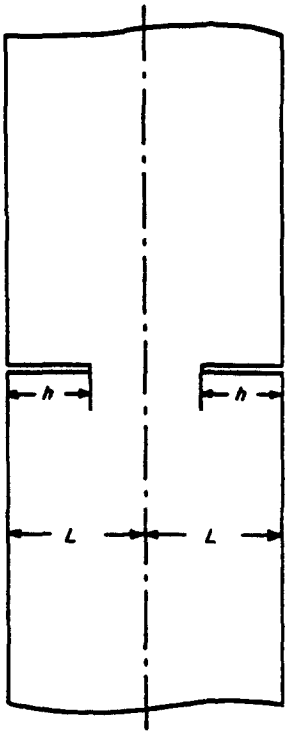

Fig. C1. Infinite strip with symmetric edge cracks.